

DATA MODELLING AND SIMULATION CONTROL OF STEAM HEAT CIRCULATION SYSTEM IN COAL-FIRED POWER PLANT

by

Shufeng ZHANG*

Suzhou Industrial Park Institute of Services Outsourcing, Suzhou, Jiangsu, China

Original scientific paper
<https://doi.org/10.2298/TSCI2104983Z>

To make up for the lack of domestic research on the dynamic model of the unit in a gas-steam combined cycle power plant, the thesis researched and established a real-time digital simulation model of the combined cycle power plant unit. Firstly, the theory found a non-real-time digital simulation model in MATLAB/SIMULINK environment. Then the paper converts it into C language code and uses the C Builder tool to encapsulate it into a simulation model that can run in real-time. Finally, the thesis conducted a simulation test on the model on real-time digital simulation and compared it with the field test results. The simulation results show that the combined cycle power plant unit model we have established can meet the real-time simulation requirements of the power system in terms of computational efficiency and model accuracy.

Key words: combined cycle power plant, modelling, real-time digital simulation, encapsulation model

Introduction

The gas-steam combined cycle power generation technology is a clean power generation technology with high efficiency, low pollution, low water consumption, fast start-up, and large capacity. The combined cycle power plant (CCPP) unit consists of four parts: gas turbine, steam engine, waste heat boiler, and generator. The working principle of the CCPP unit is to superimpose the Brayton cycle of the gas turbine operating in the high temperature zone and the Rankine cycle of the steam engine running in the medium and low temperature area to form a combined power generation system. Since the CCPP unit makes full use of the gas turbine's high average heat absorption temperature, its unit efficiency can reach about 60%. The working efficiency of CCPP units is significantly higher than that of gas-fired units and steam units. In addition the advantages of high power generation efficiency and less environmental pollution, CCPP units also have excellent load regulation performance. Its theoretical variable load rate can reach 10% MCR per minute (MCR, maximum continuous output). It can get 5% MCR per minute in practical applications, which is far superior to the regulation characteristics of conventional coal-fired units at 2% MCR per minute. In the future smart grid, this adjustment capability will play an essential role in smoothing the volatility of RES such as wind [1].

Strengthening the exploration, exploitation, and application of natural gas and developing green and low carbon technologies and recycling technologies have become an essential national policy of our country. By 2020, Chinese natural gas industry can provide sufficient fuel for 160 million kW gas-steam combined cycle power plants. The development of a combined

* Author's e-mail: zhangshuf@siso.edu.cn

cycle is of great significance to improving the domestic environment and adjusting the national energy structure. However, the current research on the dynamic model of CCPP units is still minimal. Domestic research on the combined cycle is mainly based on simulation modelling from the perspective of thermodynamics. When the CCPP unit model is needed in the grid analysis and research, we often replace it with a gas-fired unit or a steam unit model. In standard power systems simulation software such as RTDS, PSCAD, PSS/E, and Dig Silent, there is a general lack of models for CCPP units.

In response to the previous problems, this paper takes the 9F-class heavy-duty gas-steam CCPP unit widely used in China as the object. It establishes a real-time digital simulation model of the single-shaft combined-cycle unit on the RTDS platform. At the same time, we used the C Builder tool to encapsulate the simulation model to improve the reusability of the model.

Gas-steam combined cycle unit modelling

For the single-shaft unit type, the sliding pressure non-compensated waste heat boiler is used in this paper. The model established in this paper is shown in fig. 1.

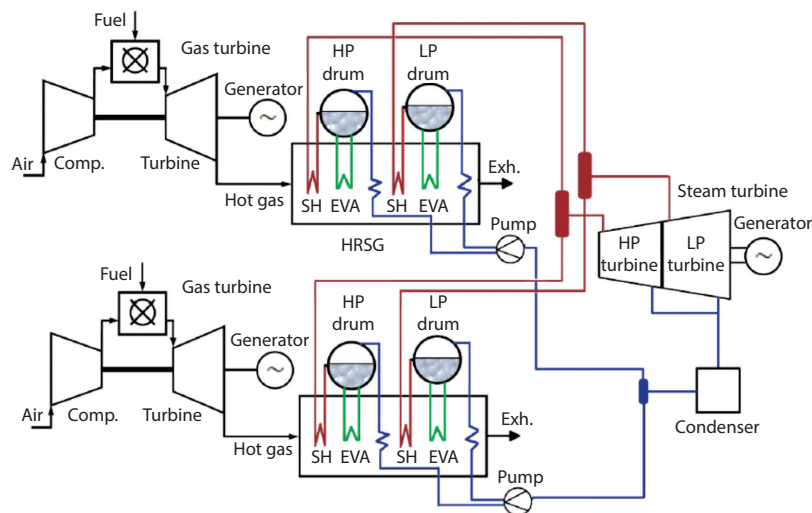


Figure 1. Simulation model of combined cycle unit

We consider three dynamic control loops in the gas turbine model: acceleration control, temperature control, and speed control. Among them, we use proportional-integral (PI) control for speed and temperature control. We use integral control for acceleration control, fig. 1. The input of speed control is electromagnetic power, speed, and the reference value of rate. The intake of temperature control is the measured temperature and temperature reference value. The information of acceleration control is the reference value of speed and acceleration. In the sliding pressure operation mode, the power output of the steam turbine follows that of the gas turbine. The output ratio of the gas turbine and the steam turbine is close to 2:1. The power output of the CCPP unit without supplementary combustion of the waste heat boiler in steady-state operation is determined by the output power of the gas turbine. Under dynamic conditions, the overall load response speed of the unit is mainly limited by the waste heat boiler. In the simulation model, we use the standard unit value, and the CCPP model finally outputs the total mechanical torque to the generator. The generator uses the apparent power (MVA) as

the reference value, and the prime mover uses the rated power (MW) as the reference value. There are three mechanisms for heat transfer to heat absorption: good thermal quality, ground formation through conduction, and ground formation through convection. Among them, the formula is expressed:

$$\frac{\partial \theta_w}{\partial \tau_s} + \frac{\partial \theta_w}{\partial \zeta} + NTU(\tau_s)\theta_w + \frac{Pe_x}{Pe_z} \frac{2H}{\pi R_0} \left[\theta_w - \frac{1}{\pi} \int_{\pi/2}^{3\pi/2} \theta_{well}(\varphi, Pe_x, \tau_s) d\varphi \right] = 0 \quad (1)$$

where θ_w is the scale temperature of healthy water, k_g – the thermal conductivity of the formation, and $\zeta = z/H$ is used to measure the Z-direction. In proportion:

$$\tau_s = \frac{m_w C_{pw} t}{\rho_w C_{pw} V} = \frac{t}{t^*} \quad (2)$$

$$Pe_i = \frac{\rho_w C_{pw} U_i R_0}{k_g} \quad (3)$$

$$NTU(\tau_s) = \frac{(hA)_e}{m_w C_{pw}} \quad (4)$$

$$\frac{\partial \theta_e}{\partial \tau_s} + \frac{\partial \theta_e}{\partial \zeta} = 0 \quad (5)$$

where θ_e is the temperature on the early time scale. The solution of eq. (5) is:

$$\theta_e(\zeta, \tau_s) = \frac{2}{Pe_z} \frac{H}{R_0} \left(1 - \frac{\zeta}{\tau_s} \right), \quad \tau_s \leq 1, \quad 0 \leq \zeta \leq \tau_s \quad (6)$$

The heat conversion problem is solved through the backflow and annular flow of the typical system return pipe. Therefore, the eq. (6) can be expressed:

$$\theta_e(\zeta, \tau_s) = \frac{2}{Pe_z} \frac{H}{R_0} \left(1 - \frac{\zeta}{\tau_s} \right) + f_{sc}(\zeta, \tau_s) \quad (7)$$

where $f_{sc}(\zeta, \tau_s)$ is A function, which is a return pipe-line from global energy balance:

$$Q_{sc} = m_w C_{pw} \Delta T_{sc} = (UA)_{sc} \Delta T_{w \rightarrow r} \quad (8)$$

Suppose the solution of the average temperature change of the return pipe flowing from the annulus is:

$$f_{sc}(\zeta, \tau_s) = \frac{\Delta T_{sc}}{Q} = \frac{1}{2\pi H k_g} \frac{H}{R_0} \frac{(UA)_{sc}}{m_w C_{pw}} \left(1 - \frac{\zeta}{\tau_s} \right), \quad \tau_s \leq 1, \quad 0 \leq \zeta \leq \tau_s \quad (9)$$

The hot well temperature in the and Z-directions is kept constant and given.

Under the condition $\tau_s > 1$, we require the temperature of the hot well in the Z-direction be kept constant:

$$\theta_e(\zeta) = \frac{2}{Pe_z} \frac{H}{R_0} (1 - \zeta) + \frac{1}{Pe_z} \frac{H}{R_0} \frac{(UA)_{sc}}{m_w C_{pw}} (1 - \zeta) \quad (10)$$

Speed control

Figure 1 contains the speed control. It is the essential part of the gas turbine control. We choose the appropriate parameters K_{pg} and K_{ig} to adjust the response speed of the gas turbine. The parameter d_{bd} can adjust the power fluctuation dead zone range and the parameter L_{set} is the speed/load reference. It can be adjusted in response to the AGC command P_{AGC} to change the base load of the unit [2].

Acceleration control

Acceleration control controls the combustion system when the speed change rate of the unit exceeds the limit. This control is significant in the process of unit start-up or load shedding. The acceleration is controlled by the integral coefficient, K_{ia} , according to the reference value a_{set} .

Temperature control

When the gas turbine exhaust gas temperature exceeds the limit, the temperature control starts to work. Temperature control consists of three parts: a temperature measurement module, a comparison module, and PI controller. The parameter T_{thcp} , T_n , and T_d in the temperature measurement module represents the influence of the thermocouple and the radiation shielding layer on the measurement process. The $F(x)$ is a non-linear function reflecting the impact of speed on temperature control. Parameter T_{limit} is the temperature limit value. The difference between the measured temperature and T_{limit} is adjusted by the PI controller, and their proportional-integral coefficients are K_{pt} and K_{it} , respectively.

Steam turbine control

Since this model uses a non-compensated waste heat boiler and sliding pressure operation mode, the control of the steam turbine is relatively simple. The parameter T_{drum} represents the time constant of the waste heat boiler, which reflects the response speed of the waste heat boiler. The $F(P_{gt})$ represents the non-linear mapping relationship between the heat Q_g absorbed by the waste heat boiler and the output power, P_{gt} , of the gas turbine. The P_t represents the primary steam pressure of the inlet valve of the steam turbine. The P_{ref} represents the minimum steam pressure reference value. When P_{ref} is very small, the speed governing system of the steam turbine does not work. At this time, the regulating valve fully open system realizes sliding pressure operation [3].

Combined cycle encapsulation model based on C Builder

The C Builder component development based on SIMULINK

The RTDS is a set of devices using multi-CPU parallel processing technology. Its EMTP model can simulate the electromagnetic transient process of the power system. At present, RTDS is the most mature and widely used real-time digital simulation system in the world. The RTDS can carry out real-time simulation and form a flexible and convenient digital-physical closed loop with external equipment. The RTDS simulation of primary equipment can make the parameters consistent with the existing system.

All control components and their parameters in RTDS are global. If we only use the control components to build the CCPP unit model in fig. 1, the constructed model is challenging to instantiate multiple times and cannot be reused modularly. To solve this problem, we can use the component customization C Builder provided by RTDS to encapsulate the control model. The encapsulated system has many advantages: a straightforward input/output interface can be instantiated multiple times, higher execution efficiency, and so on [4]. But C Builder requires

manual programming of C language to realize the control model, and it is not easy to debug the control model in the C Builder environment. The MATLAB/SIMULINK provides an efficient controller modelling and debugging environment, which can help us convert SIMULINK models into high performance ANSIC codes that support floating-point operations to achieve the purpose of running on the host's real-time embedded platform. The processor chip used in the RTDS system is IBM Power PC 750 GX or Freescale Power PC MPC 7448. Suppose the processor, as mentioned previously, is regarded as the host embedded platform for SIMULINK to generate code. In that case, we can carry out rapid model development and testing in the SIMULINK environment, and then we will migrate the model to the RTDS platform. The aforementioned product as process is shown in fig. 2.

The CCPP component interface definition

First, we need to define the external interface of the CCPP component. The CCPP component interface defined in this paper is shown in fig. 3, and its port is defined:

- P_{MAC} : input port. It is the output electromagnetic power from the generator.
- L_{set} : input port. It is the reference value of unit load/speed.
- W : input port. It is the speed of the generator.
- TM : output port. It is the mechanical torque input to the generator.

Besides, this article also defines the parameters that can be configured for CCPP components. For specific parameter items, see the simulation test part of this article [5].

The SIMULINK model development and automatic code generation

According to the previous interface definition, we use SIMULINK to complete the development of the CCPP model shown in fig. 1 [6]. The simulation step size of the model should be set to fixed step size. Then we use SIMULINK/EMBEDDED Coder to generate ANSIC code, as shown in tab. 1 automatically.

Table 1. The SIMULINK generated by the main source code

The filename	The file
CCPP_Sim_data.c	Contains the initial parameter values used by the model
CCPP_Sim_private.h	Contains the definition of a private instruction that accesses the real-time model
CCPP_Sim_types.h	Contains definitions of the data types used in the model
CCPP_Sim.c	Main files for implementing CCPP model functions
CCPP_Sim.h	Contains model parameters and state variable definitions

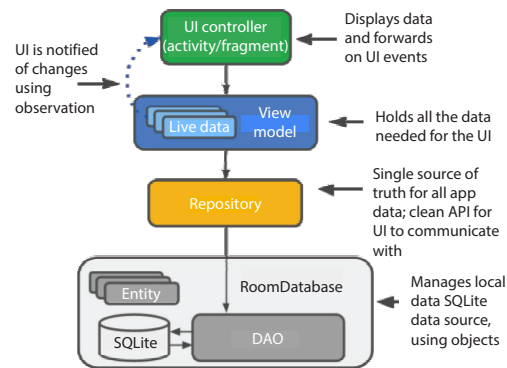


Figure 2. The C Builder component development process based on SIMULINK

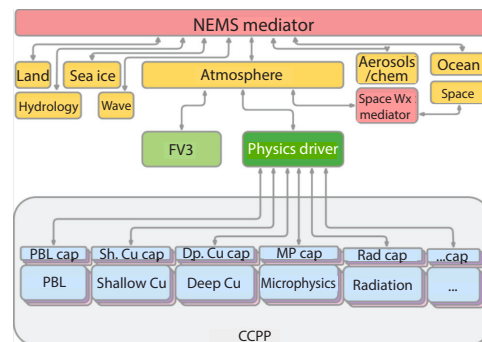


Figure 3. Interface definition for the CCPP component

The C Builder component creation and integration compilation

The article uses RTDS/C Builder to create CCPP components with the same interface and generate ANSIC code. However, the code only contains interface definitions but not function implementations. The function realization needs to import the function code generated by SIMULINK to form all the source codes required to build the CCPP model on the RTDS platform. We can integrate and compile the aforementioned code to develop a CCPP model packaged as a custom component. This model can be reused in RTDS.



Figure 4. Test system

Simulation test

We use RTDS to establish the test system shown in fig. 4. The rated power of the unit is 400 MW, and the generator capacity is 470 MVA. The figure shows the connection relationship between the CCPP component developed in this paper and the generator [7].

Open the parameter configuration dialog box of the CCPP component to configure the parameter items shown in tab. 2.

Table 2. Main parameters of the combined cycle model

Parameter names	The values	Parameters to describe
R_p	0.045	Coefficient of gas turbine adjustment
K_{pg}	4	Proportional coefficient of the governor
K_{ig}	1.5	Governor integral coefficient
K_{ia}	10	Acceleration control integral coefficient
K_{pt}	1	Temperature controlled amplification factor
K_{it}	0.2	Temperature control integral coefficient
W_{fo}	0.2 p.u.	Full speed no-load fuel
K_{gt}	0.65	Gas turbine power distribution coefficient
T_{drum}	300 seconds	Waste heat boiler time constant
P_{ref}	0.3 p.u.	Minimum vapor pressure reference value

Step disturbance test of combined cycle frequency

The same test method is used in the simulation in this article. The unit carries a frequency step disturbance experiment with more than 80% load stably. The comparison between actual measurement results and simulation results is shown in fig. 5, and the two are the same [8]. The gas turbine output simulation results are the same as the measured results, but when the frequency returns to 50 Hz, the simulated output is about 3MW less than the measured output. This is because there is a dead speed zone in the gas turbine speed control process, and the allowable power has an error of ± 2.4 MW. The simulation result of the steam turbine output response is slower than the measured result. The simulated output during the dynamic process is about 1MW more power output than the actual measured output. The simulation results of the entire output trajectory of the CCPP unit agree with the measured results.

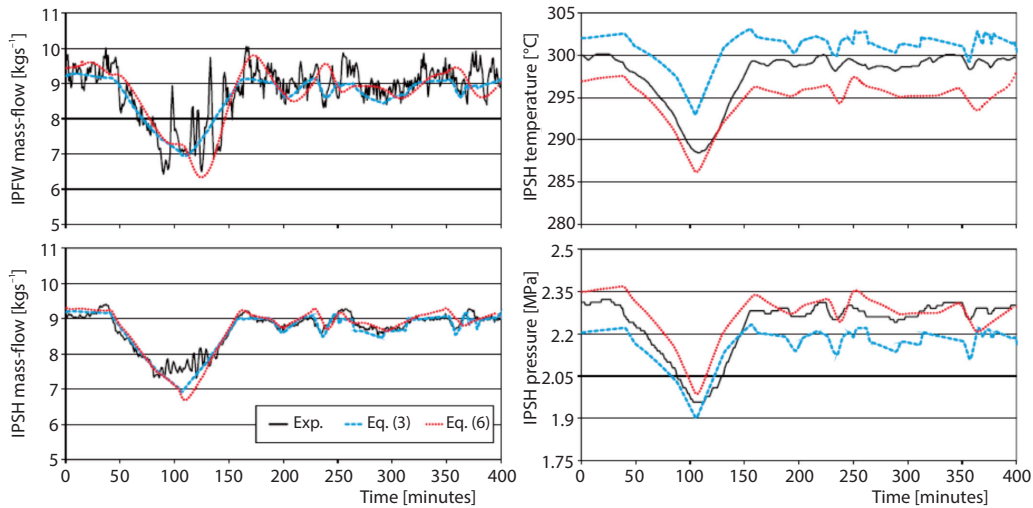


Figure 5. Joint cycle frequency step disturbance test

Test for dynamic characteristics of combined cycle frequency

When the unit was at 80% load, we suddenly cut off the 50 MW bag. The unit output was reduced from the initial 320 MW to 270 MW, and the system frequency stabilized at 50.25 Hz after experiencing disturbance from 50 Hz. The frequency change process is shown in fig. 6. From fig. 6, the characteristic droop slope of the governor can be calculated to be 4%. This point is consistent with the distinct droop slope of the actual unit.

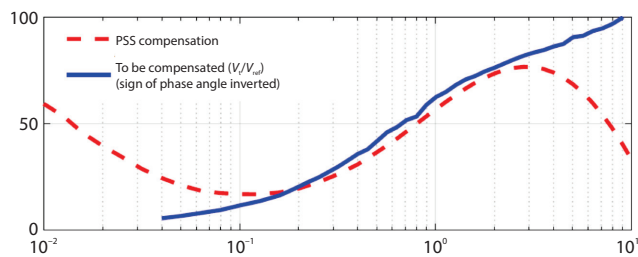


Figure 6. Dynamic characteristic test of combined cycle frequency

Acceleration control test

When the unit was at 95% load, we suddenly cut off the 120 MW bag, and the unit output was reduced from the initial 380 MW to 240 MW. In the initial stage of load shedding, the generator rotor acceleration is positive. When the acceleration exceeds the acceleration setting value, the acceleration control starts to work to reduce the acceleration control amount [9]. When the acceleration control quantity is less than the speed control quantity, the acceleration control plays a significant role in controlling the fuel. The acceleration control process of the CCPP unit is shown in fig. 7.

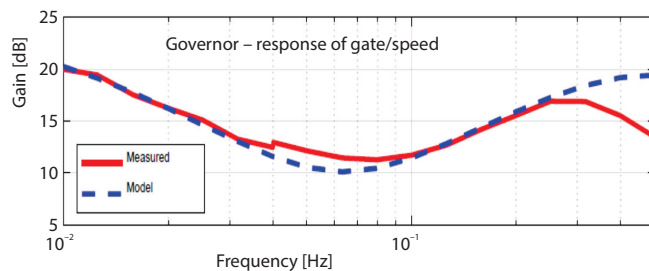


Figure 7. Combined cycle acceleration control test

Real-time computing efficiency test of the model

We used a processor in the GPC processor card during the test. The processor chip is IBMPPC750GX, clocked at 1 GHz. We use the RTDS performance test tool to measure the time required for the CCPP model to run at about 5.5 μ s. If the system simulation step is 50 μ s, then a single RTDS processor can run up to 9 CCPP unit models simultaneously. This shows that the model has good real-time calculation efficiency [10].

Conclusion

As a form of clean power generation in the future smart grid, CCPP units can be operated in coordination with other random renewable energy sources. According to the actual operation of CCPP units in China, this paper developed a combined cycle simulation model including a gas turbine, waste heat boiler, and steam turbine on RTDS. The effectiveness of the model is verified by comparison with the actual measurement results of the unit.

References

- [1] Kumar, R. Thermodynamic Modelling and Validation of a 210-MW Capacity Coal-Fired Power Plant, *Iranian Journal of Science and Technology, Transactions of Mechanical Engineering*, 40 (2016), 3, pp. 233-242
- [2] Kumar, S., *et al.*, Energy and exergy analysis of a coal fired power plant. Mehran University Research *Journal of Engineering and Technology*, 37 (2018), 4, pp. 611-624
- [3] Wu, S., Study and Evaluation of Clustering Algorithm for Solubility and Thermodynamic Data of Glycerol Derivatives, *Thermal Science*, 23 (2019), 5, pp. 2867-2875
- [4] Li, Y. H., *et al.*, A Novel Dual-Bed for Steam Gasification of Biomass, *Biomass Conversion and Biorefinery*, 8 (2018), pp. 357-367
- [5] Wu, X., *et al.*, Investigation of Characteristics of Passive Heat Removal System Based on the Assembled Heat Transfer Tube, *Nuclear Engineering and Technology*, 48 (2016), 6, pp. 1321-1329
- [6] Xiao, Y., *et al.*, Catalytic Steam Co-Gasification of Biomass and Coal in a Dual Loop Gasification System with Olivine Catalysts, *Journal of the Energy Institute*, 93 (2020), 3, pp. 1074-1082
- [7] Pleshanov, K. A., *et al.*, Design of a Natural Circulation Circuit for 85 MW Steam Boiler, *Thermal Science*, 21 (2017), 3, pp. 1503-1513
- [8] Juangsa, F. B., Aziz, M., Integrated System of Thermochemical Cycle of Ammonia, Nitrogen Production, and Power Generation, *International Journal of Hydrogen Energy*, 44 (2019), 33, pp. 17525-17534
- [9] Shaofei, Wu., Construction of Visual 3-D Fabric Reinforced Composite Thermal Performance Prediction System, *Thermal Science*, 23 (2019), 5, pp. 2857-2865
- [10] Kim, S., *et al.*, Dynamic Simulation of a Circulating Fluidized Bed Boiler System – Part I: Description of the Dynamic System and Transient Behavior of Sub-Models, *Journal of Mechanical Science and Technology*, 30 (2016), 12, pp. 5781-5792